Journal of Neurochemistry

JOURNAL OF NEUROCHEMISTRY | 2016

doi: 10.1111/jnc.13651

ORIGINAL ARTICLE

Post-ischemic salubrinal treatment results in a neuroprotective role in global cerebral ischemia

Berta Anuncibay-Soto,* Diego Pérez-Rodríguez,* María Santos-Galdiano,* Enrique Font,* Marta Regueiro-Purriños† and Arsenio Fernández-López*

*Área Biología Celular, Instituto Biomedicina, Universidad de León, León, Spain

†Department Cirugía Medicina y Anatomia Veterinaria, Universidad de León, León, Spain

Abstract

This study describes the neuroprotective effect of treatment with salubrinal 1 and 24 h following 15 min of ischemia in a two-vessel occlusion model of global cerebral ischemia. The purpose of this study was to determine if salubrinal, an enhancer of the unfolded protein response, reduces the neural damage modulating the inflammatory response. The study was performed in CA1 and CA3 hippocampal areas as well as in the cerebral cortex whose different vulnerability to ischemic damage is widely described. Characterization of proteins was made by western blot, immunofluorescence, and ELISA, whereas mRNA levels were measured by Quantitative PCR. The salubrinal treatment decreased the cell demise in CA1 at 7 days as well as the levels of matrix metalloprotease 9 (MMP-9) in CA1 and cerebral cortex at 48 h and ICAM-1 and VCAM-1 cell adhesion molecules. However, increases in tumor necrosis factor α and nuclear factor kappa-light-chain-enhancer of activated B cells (NF-κB) inflammatory markers were observed at 24 h. Glial fibrillary acidic protein levels were not modified by salubrinal treatment in CA1 and cerebral cortex. We describe a neuroprotective effect of the post-ischemic treatment with salubrinal, measured as a decrease both in CA1 cell demise and in the blood–brain barrier impairment. We hypothesize that the ability of salubrinal to counteract the CA1 cell demise is because of a reduced ability of this structure to elicit unfolded protein response which would account for its greater ischemic vulnerability. Data of both treated and non-treated animals suggest that the neurovascular unit present a structure-dependent response to ischemia and a different course time for CA1/cerebral cortex compared with CA3. Finally, our study reveals a high responsiveness of endothelial cells to salubrinal in contrast to the limited responsiveness of astrocytes.

Keywords: BBB impairment, inflammation, ischemia, salubrinal, UPR.

J. Neurochem. (2016) 10.1111/jnc.13651

Stroke is reported to be one of the major causes of death, the leading cause of permanent disability and the second-ranked cause of dementia in developed countries (Donnan *et al.* 2008; World Health Organization (WHO) 2011). Its main cause is a reduction in blood flow (ischemic stroke) that leads to an impairment in neural tissue homeostasis. The extent of brain damage after stroke depends on the ability of the brain to recover homeostasis (Posada-Duque *et al.* 2014; Doll *et al.* 2015). At the cellular level, ischemia results in accumulation of unfolded proteins in the endoplasmic

Received February 17, 2016; revised manuscript received April 7, 2016; accepted April 19, 2016.

Address correspondence and reprint requests to Arsenio Fernández López, Área de Biología Celular, Instituto de Biomedicina, Universidad de León, León, Spain. E-mail: aferl@unileon.es

Abbreviations used: 24IR-Sal, Experimental group of animals with 15 min of ischemia and 24 h of reperfusion, treated with salubrinal; 24IR-Vehicle, Experimental group of animals with 15 min of ischemia and 24 h of reperfusion, treated with vehicle; 24S-Sal, Sham-operated animals killed 24 h after surgery, treated with salubrinal; 24S-Vehicle, Sham-operated animals killed 24 h after surgery, treated with vehicle; 48IR-Sal, Experimental group of animals with 15 min of ischemia and 48 h of reperfusion, treated with salubrinal; 48IR-Vehicle, Experimental group of animals with 15 min of ischemia and 48 h of reperfusion, treated with vehicle; 48S-Sal, Sham-operated animals killed 48 h after surgery, treated with salubrinal; 48S-Vehicle, Sham-operated animals killed 48 h after surgery, treated with vehicle; BBB, blood–brain barrier; CA, Cornu Ammonis; CAM, Cell adhesion molecules; Cx, Cerebral cortex; DAPI, 4′,6-diamidino-2-phenylindole; eIF2α, Eukaryotic initiation factor 2α; ER stress, Endoplasmic reticulum stress; GFAP, glial fibrillary acidic protein; I/R, Ischemia/reperfusion; ICAM-1, intercellular adhesion molecule 1; MMP-9, matrix metalloprotease 9; NF-κB, nuclear factor kappa-light-chain-enhancer of activated B cells; PERK, protein kinase RNA-like endoplasmic reticulum kinase; TBST, Tris-buffered saline 50 mM with 0.2% Tween 20; TNF-α, tumor necrosis factor α; UPR, unfolded protein response; VCAM-1, vascular adhesion molecule 1.

reticulum (ER stress). This elicits the so-called unfolded protein response (UPR), which attempts to restore cell homeostasis and prevent cell death (Kaufman 1999; Walter and Ron 2011). At a systemic level, ischemia elicits a protective inflammatory response whose excess results in the so-called sterile inflammation that contributes to increase the neural damage (Ceulemans *et al.* 2010; Corps *et al.* 2015). Much evidence supports the crosstalk between UPR and inflammation, suggesting new targets for stroke therapies (Aarts *et al.* 2003; Zhang and Kaufman 2008; Hasnain *et al.* 2012).

The ischemia-induced inflammatory response has been reported to modify the blood–brain barrier (BBB), also called the neurovascular unit (Hawkins and Davis 2005). Inflammation contributes to BBB impairment by increasing the expression of the cell adhesion molecules (CAMs) in the endothelium (Jin *et al.* 2010), as well as promoting the release of matrix metalloproteases. These enzymes degrade the extracellular matrix and assist leukocyte migration through the endothelium, allowing blood proteins to extravasate into the cerebral parenchyma (Wang *et al.* 2007; Yilmaz and Granger 2010). In turn, this increases the BBB permeability and the inflammatory response, increasing the ischemia-induced damage.

One key marker of inflammation is tumor necrosis factor α (TNF-α), the major pro-inflammatory cytokine (Joussen *et al.* 2009), which ignites the canonical nuclear factor kappa-light-chain-enhancer of activated B cells (NF-κB) activation and is considered the main pathway in the inflammatory response (Rius *et al.* 2008). TNF-α promotes the expression of CAMs and matrix metalloproteases and is also a strong inducer of ER stress (Xue *et al.* 2005; Li *et al.* 2011). In turn, ER-stress is able to induce a non-canonical activation of NF-κB, inhibiting the canonical NF-κB activation induced by the inflammatory stimuli (Kitamura 2009; Nakajima and Kitamura 2013). The earlier UPR pathway is activated by protein kinase RNA-like endoplasmic reticulum kinase (PERK) (Nakka *et al.* 2014). The PERK pathway is characterized by eIF2α phosphorylation (Schroder and Kaufman 2005; Schroder 2008), which leads to a general blocking of protein translation (Harding *et al.* 2000; Fernandez *et al.* 2002). The eIF2α phosphorylation has been reported to be the necessary and sufficient requirement for the non-canonical ER-stress-dependent activation of NF-κB (Jiang *et al.* 2003; Deng *et al.* 2004). Salubrinal, an inhibitor of phosphatase PP1, blocks the dephosphorylation of eIF2α (Boyce *et al.* 2005), thus enhancing the PERK pathway. This enhancement could be a protective therapeutic strategy to prevent vascular inflammation (Halterman *et al.* 2008; Li *et al.* 2011). In fact, treatment with salubrinal prior to ischemic insult presents a neuroprotective effect (Nakka *et al.* 2010) and a recent study has also demonstrated a neuroprotective role of salubrinal in traumatic brain injury (Rubovitch *et al.* 2015).

We hypothesize that the enhancement of UPR would reduce both ER stress and the inflammatory response, thus reducing the ischemic damage. In this report, we demonstrate for the first time the neuroprotective role of salubrinal treatment administered after an ischemic insult and show that this agent modifies the inflammatory response triggered by ischemia. We also show that ischemic insult induces structure-dependent differences in the BBB permeability.

Material and methods

Animals

Sixty-three-month-old Sprague–Dawley male rats (350–450 g) were housed at standard temperature (22 ± 1°C) in a 12 h light/dark cycle with food (Panlab, Barcelona, Spain) and water *ad libitum*. The experimental groups were set up as indicated in Table 1.

All experimental procedures were carried out in compliance with the ARRIVE guidelines, in accordance with the Guidelines of the European Union Council (63/2010/EU) following Spanish regulations (RD 53/2013, BOE 8/2/2013) for the use of laboratory animals and were approved by the Scientific Committee of the University of Leon. All efforts were made to minimize animal suffering and to reduce the number of animals used.

Transient global cerebral ischemia

Animals injured following a two-vessel occlusion global cerebral ischemia model (IR) and their corresponding sham-operated controls (without carotid clamping) were obtained following the procedure previously described (Vieira *et al.* 2014). Briefly, induction of anesthesia was carried out with 4% isoflurane (IsoFlo, Abbott Laboratories Ltd, Madrid, Spain) in 3 L/min in 100% oxygen and then animals were maintained under anesthesia with a flux of 1.5–2.5% isoflurane at 800 mL/min in 100% oxygen, through a face mask. After exposing both carotid arteries, the femoral artery was exposed and catheterized to record blood pressure along the whole procedure. This pathway was also used to maintain a moderate hypotension (40–50 mm Hg) by partial exsanguination (about 8 ml of blood slowly extracted at 1 ml/min) to prevent the blood flow to the brain through the paravertebral arteries. To prevent clot formation, 50 UI heparin/kg was supplied to the animal through this catheter and 50 UI heparin were maintained in 3 mL saline in the syringe used for

Table 1 Experimental conditions

Time of IR	Sham animals		Ischemic animals	
5 h			Treated (5IR-Sal)	Vehicle (5IR-Vehicle)
24 h	Treated (24S-Sal)	Vehicle (24S-Vehicle)	Treated (24IR-Sal)	Vehicle (24IR-Vehicle)
48 h	Treated (24S-Sal)	Vehicle (24S-Vehicle)	Treated (48IR-Sal)	Vehicle (48IR-Vehicle)
7 days		Vehicle (7D-S)	Treated (7DIR-Sal)	Vehicle (7DIR-Vehicle)

storing extracted blood. When hypotension values were stable, the transient global ischemia was induced by clamping both common carotid arteries for 15 min. Temperature of the body was maintained at 36 ± 1°C during surgery with a feedback-regulated heating pad using a rectal probe. After ischemia, blood was returned to the animal at 1 mL/min until the arterial blood pressure recovered. After removing the catheter, the animal was sutured and once consciousness returned it was transported to an air-conditioned room at 22 ± 1°C until killed. The same procedure was carried out in sham-operated rats, except the carotid arteries clamping.

Salubrinal treatment

One hour after surgery, all animals were injected intraperitoneally either with 1 mg/kg of salubrinal (TOCRIS, Bristol, UK) in saline with 1.5% dimethylsulfoxide, or vehicle. Animals with 48 h and 7 days of IR were injected with a second dose of salubrinal or vehicle 24 h after surgery.

Tissue dissection and total RNA and protein extraction

After decapitation, brains were quickly removed and placed on a brain rodent matrix (ASI Instruments, Warren, MI, USA) at 4°C to obtain 2-mm-thick sagittal slices at a distance of 1 mm to the medial line. *Cornu Ammonis 1* (CA1) and *Cornu Ammonis* 3 (CA3) hippocampal regions, as well as the cerebral cortex (Cx) above them, were dissected under a light microscope. Samples were frozen in dry ice and stored at −80°C. Total RNA and protein were extracted from each dissected brain region using the Tripure Isolation Reagent® (Roche Diagnostics, Barcelona, Spain) following the manufacturer's instructions and then stored at −80°C.

Reverse transcriptase reaction and qPCR

All Quantitative PCR (qPCR) assays in this study were performed following the Minimal Information for Publication of Quantitative Real-Time PCR Experiments (MIQE) Guidelines (Taylor *et al.* 2010). RNA integrity and retrotranscription was performed as previously described (Anuncibay-Soto *et al.* 2014). qPCR was performed in a Step One Plus thermocycler (Applied Biosystems, Foster City, CA, USA) using the following primers: MMP-9: (f5′ttctgtccagaccaagggtaca, r5′gcgcatggccgaactc, NM_ 031055.1); vascular adhesion molecule 1 (VCAM-1): (f5′tgctcctgacttgcagcaccac, r3′tgtcatcgtcacagcagcaccc, NM_ 012889.1); intercellular adhesion molecule 1 (ICAM-1): (f5′tgcagccggaaagcagatggtg, r3′atggacgcc acgatcacgaagc, NM_012967.1); glyceraldehyde 3-phosphate dehydrogenase (GAPDH): (f5′gggcagcccagaacatca, r3′tgaccttgcccacagcct, NM_017008).

Optimal qPCR conditions in our assays were obtained using 2 µL of 1/10 cDNA and 300 nM of, using SYBR Green Master Mix as the fluorescent DNA dye (Applied Biosystems). The results were analyzed following the $2^{-\Delta\Delta Ct}$ method (Livak and Schmittgen 2001), using *gapdh* housekeeping gene as a reference to normalize the Ct values for each gene to be analyzed. Fold changes were expressed as $2^{-\Delta\Delta Ct}$, where ΔΔCt represents the transcript variation between the different conditions $(\Delta Ct_{ischemic} - \Delta Ct_{sham})$ and $(\Delta Ct_{salubrinal} - \Delta C_{tvehicle})$.

Western blot analysis

Protein samples were resuspended in 8 M urea with 4% sodium dodecyl sulfate in the presence of a protease inhibitor (complete protease inhibitor cocktail EDTA free; Applied Biosystems) and quantified using a DC Protein Assay Kit (Bio-Rad, Hercules, CA, USA). Band gels were obtained from 25 µg of each sample as previously described (Anuncibay-Soto *et al.* 2014) using the following primary antibodies: NF κB raised in rabbit (Abcam, Cambridge, UK, 1 µg/mL); MMP-9 raised in rabbit (Abcam, 1 µg/mL); ICAM-1 raised in rabbit (Abcam, 0.75 µg/mL); GFAP raised in rabbit (Dako, Glostrup, Denmark, 1 µg/mL); TNF-α raised in rabbit (Abcam, 1 µg/mL) and β-actin raised in mouse (Sigma Aldrich, Madrid, Spain, 0.2 µg/mL).

The resulting bands were digitalized in a GS-800 Calibrated Densitometer (Bio-Rad) and band optical densities were quantified with ImageJ Software (NIH, Washington, MD, USA). The corresponding β-actin bands were used to normalize the optical density of the bands.

Immunofluorescence assays

Another 15 rats with 7 days of reperfusion were killed with an intraperitoneal dose of 200 mg/kg of sodium pentobarbital (Vetoquinol, Vernois, France) and immediately perfused via intra-aortic delivery of 4% paraformaldehyde as previously described (Anuncibay-Soto *et al.* 2014). Fixed brains were cut in 40-µm-thick coronal sections for immunohistochemical assays.

An epitope-retrieval step was conducted transferring the sections to 0.05% Tween-20 in 10 mM sodium citrate buffer, pH 6.0, at 80°C for 30 min followed by blocking in 20% goat serum with 0.2% TritonX-100 in phosphate-buffered saline for 1 h at 21°C. Sections were incubated overnight at 4°C with anti-NeuN antibody raised in mouse (1 : 500) (Millipore, Darmstadt, Germany) and then with a rabbit anti-mouse IgG conjugated with Alexa-568 (1 : 500)(Life Technologies, Carlsbad, CA, USA). Nuclei were counter-stained with 4′,6-diamidino-2-phenylindole (Sigma, Madrid, Spain) and sections mounted using Fluoromount G Mounting Medium (Life Technologies). The number of cells stained with NeuN in different areas was measured following the principles of the optical dissector method (serial random sections, section sampling fraction, area sampling fraction, and thickness sampling fraction) (Gundersen *et al.* 1988; Zarow *et al.* 2005). Six equidistant non-overlapping 40-µm-thick sections between Bregma −1.8 to −4.3 mm (rostro-caudal axis), following Paxinos and Watson (1996), were analyzed per animal using optical dissectors with 50 x 50 µm grid squares and a height of 30 µm for the fractionator volume (5 µm of both the top and the bottom of the section with putative damage from the cutting process were discarded). Five equidistant dissectors in the layer III of the frontoparietal cortex, motor area between 1 and 5 mm lateral to the midline, 5 equidistant dissectors in hippocampal CA1 and 4 in hippocampal CA3 areas were analyzed per section. Final results are expressed as the number of cells/mm3. Image acquisition was carried out with a Nikon Eclipse TE-2000 Confocal Microscope (Nikon Instruments, Amsterdam, Netherlands). Image processing and analysis were performed using ImageJ Software (NIH).

C-reactive protein

Blood samples from each animal were centrifuged at 1500 *g* for 15 min and the supernatant was frozen at −80°C until the ELISA test for C-reactive protein (RayBiotech, Norcross, GA, USA) could be performed following the manufacturer's instructions.

Statistical analysis

Graph Pad Prism 6.0 Software (Graph Pad Software Inc, La Jolla, CA, USA) was used for statistical analyses. Quantitative results are expressed as mean ± SEM. Two-way ANOVA following by Bonferroni post hoc test, one-way ANOVA following by Tukey post hoc test or Student's *t*-test followed by unpaired *t*-test were conducted setting the confidence level at 95%.

Results

Salubrinal effect on UPR-PERK pathway

The treatment previous to the ischemic insult with salubrinal has been reported to increase the eIF2α phosphorilation in the first hours after the insult (Nakka *et al.* 2010). We observed that the post-ischemic treatment with salubrinal also increased the eIF2α phosphorylation 5 h after ischemia in treated vs. non-treated insulted animals. We analyzed it to prove the UPR enhancement in the model here presented (Fig. 1a). This effect disappeared at 24 h. (Fig. 1b).

Inflammation markers

C-reactive protein, TNF-α, and NF-κB were used as inflammation parameters. C-reactive protein blood levels were measured at 48 h and appeared significantly increased as a consequence of IR. Salubrinal treatment following IR did not present significant changes (Fig. 1b). TNF-α levels were almost undetectable in Cx both at 24 and 48 h after the insult; however, hippocampal levels were noticeable at both times (Fig. 2a and b). Significant ischemia-dependent TNF-α increases were observed in CA1 comparing 48IR-vehicle with 48S-vehicle animals (Fig. 2b) and in CA3 comparing 24IR-vehicle with 24S-vehicle animals (Fig. 2a). Also, strikingly higher levels of TNF-α were observed in both structures comparing 48IR-vehicle with 24IR-vehicle animals. Interestingly, the treatment with salubrinal decreased the TNF-α levels in sham animals both at 24 and 48 h but resulted in increases that were significant in 24IR-Sal compared to 24IR-vehicle and non-significant when 48IR-Sal were compared to 48IR-vehicle animals. Significant interactions between salubrinal treatment and IR were observed in CA1 at 24 h.

NF-κB levels were detectable in all the structures studied (Fig. 2c and d). Significantly increased levels of this protein as a consequence of the IR were observed only in CA3 at 24 h. After salubrinal treatment we observed significant increases in NF-κB in Cx when comparing 24IR-Sal with 24IR-vehicle animals, and in CA1 when comparing 24S-Sal with 24S-vehicle animals (Fig. 2c). This contrasts with the significant decreases observed for 48IR-Sal with respect to 48IR-vehicle animals (Fig. 2d). The same comparisons in CA3 revealed a diametric response to that observed in Cx and CA1 with a salubrinal-dependent decrease at 24 h and a salubrinal-dependent increase at 48 h. A significant interaction between salubrinal treatment and IR was observed in Cx at 48 h.

Neurovascular unit

GFAP is used as an inflammatory marker of the brain (Wang *et al.* 2007). IR animals treated with salubrinal showed a significant decrease in their GFAP levels at 24 h in Cx and CA1 when compared with sham animals (Fig. 3a). This effect disappeared at 48 h (Fig. 3b). In turn, CA3 displayed a

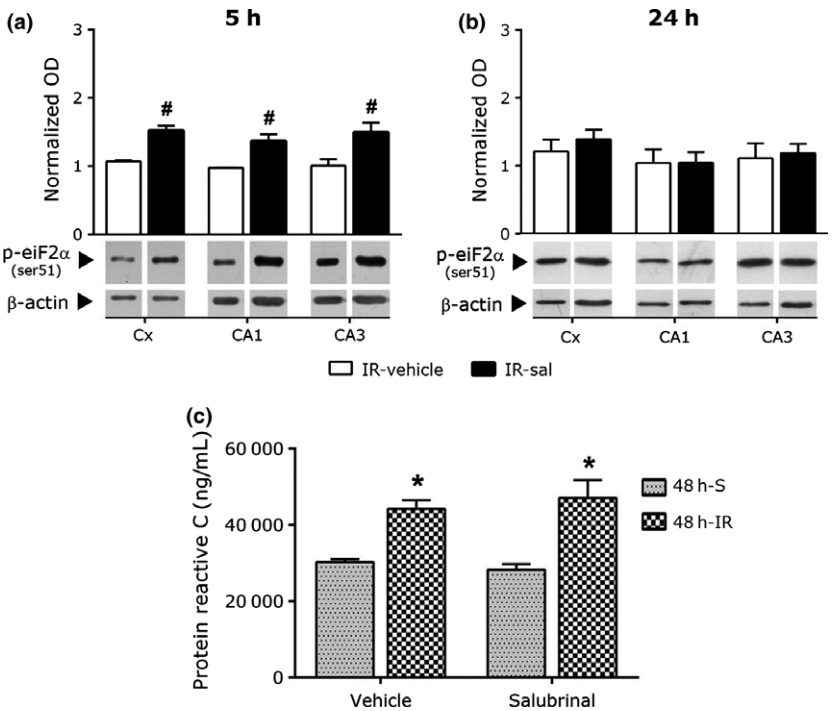

Fig. 1 Effects of salubrinal on unfolded protein response (UPR) and inflammation. Salubrinal treatment elicited an enhancement of UPR in the different structures studied but did not promote a significant effect on blood inflammation markers. Representative protein bands of (a) phosphorylated eIF2α (38 kDa) at 5 IR hours, (b) phosphorylated eIF2α (38 kDa) at 24h IR hours and (c) C-reactive protein at 48 IR hours. The averages of the densitometric analysis corresponding to five rats (mean ± SEM) normalized with respect to β-actin (40 kDa) are indicated above the bands. #indicates significant differences between the IR-Sal and IR-vehicle groups. *indicates significant differences between IR and sham in treated and non-treated animals. In all cases $p < 0.05$ by two tails unpaired Student's *t*-test, $n = 5$.

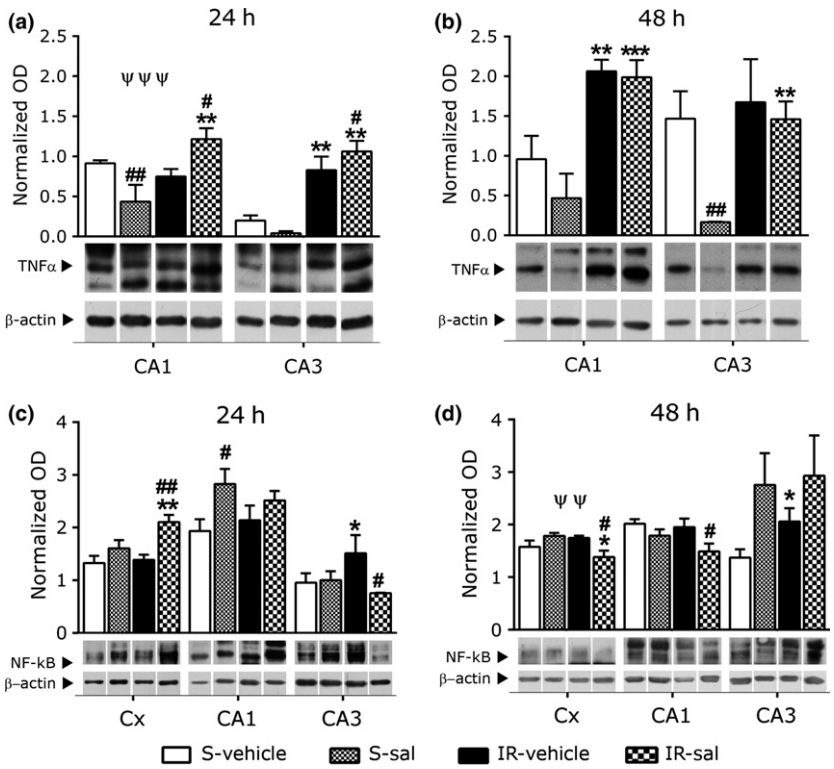

Fig. 2 Effect of IR time and treatment on protein levels of inflammatory markers. Representative protein bands of tumor necrosis factor α (TNF-α) (23 kDa) at (a) 24 h and (b) 48 h and NF-κB (55 kDa) at (c) 24 h and (d) 48 h in the different structures studied. Averages of the densitometric analysis corresponding to five rats (mean ± SEM) normalized with respect to β-actin (40 kDa) are indicated above the bands. Of note, TNF-α expression is undetectable in Cx. Statistics between the different conditions, indicated at the bottom of the image, are represented by *when IR are compared, by #when treatments are compared and by Ψfor significant interactions between IR and treatment. One symbol $p < 0.05$, two symbols $p < 0.01$, three symbols $p < 0.001$, by two-way ANOVA, $n = 5$.

different response, with no changes under the different conditions at 24 h and significant increases as a result of the ischemic insult (48 IR-vehicle vs. 48S-vehicle), in contrast with the significant decreases as a result of the salubrinal treatment (48IR-Sal compared to 48S-Sal). Also, salubrinal treatment significantly increased the CA3 GFAP protein levels in sham animals at 48 h. This effect also seemed to appear at 24 h but we failed to detect any statistical significance (Fig. 3b).

Matrix metalloproteinase 9 (MMP-9) protein levels appeared significantly increased as a consequence of the ischemia in all the structures at 48 h but only in the Cx at 24 h (Fig. 3c and d). The treatment with salubrinal resulted in significant decreases in MMP-9 levels in Cx and CA1 (48IR-Sal compared with 48IR-vehicle). Interestingly, this comparison in CA3 revealed a diametrically opposed effect with a significant salubrinal-induced increase in MMP-9 levels. A significant interaction between ischemia and salubrinal was observed in Cx at 48 h.

MMP-9 transcript level did not reveal significant differences in any of the structures studied when ischemic vehicle animals where compared to sham vehicle animals (Fig. 4a and b). The treatment with salubrinal resulted in significant MMP-9 transcript level decreases in all the structures when ischemic-treated animals were compared with the corresponding sham-treated animals at 24 h (Fig. 4a). However, at 48 h, only CA1 still showed these significant transcript decreases observed in the treated animals (Fig. 4b). Similar levels of MMP-9 transcripts were observed between sham animals treated and non-treated with salubrinal, except in CA1 at 24 h (Fig. 4c). Interestingly, these comparisons in ischemic animals revealed that salubrinal induced significant decreases in CA1 and CA3 at 24 h and in CA1 at 48 h (Fig. 4c and D).

ICAM-1 protein levels significantly increased as a consequence of the IR in CA3 at 24 h as well as in CA1 and in Cx at 48 h (Fig. 3e and f). The treatment with salubrinal in IR animals showed a trend to decrease the ICAM-1 levels in CA1 and Cx that was significant in CA3 at 24 h and in Cx at 48 h. Interestingly, the treatment with salubrinal was able to increase the ICAM-1 levels in CA3 of sham animals at 24 h, but decreased them in the Cx.

ICAM-1 transcript levels appeared significantly increased by IR in CA3 at 24 h (Fig. 5a and c) and in Cx and CA1 at 48 h (Fig. 5b and d). The treatment with salubrinal resulted in blocking or decreasing the effect of the IR both at 24 and 48 h (Fig. 5a and b). In sham animals, the salubrinal treatment did not elicit an intrinsic effect on ICAM-1 transcript levels, but decreased them significantly in all structures in 48IR animals (Fig. 5c and d). Significant interactions between salubrinal treatment and IR were observed in CA3 at 24 h and in all structures at 48 h.

VCAM-1 transcript levels increased significantly as a consequence of IR in Cx and CA1 at 48 h but only in Cx at 24 h. These ischemia-induced increases in VCAM-1 mRNA

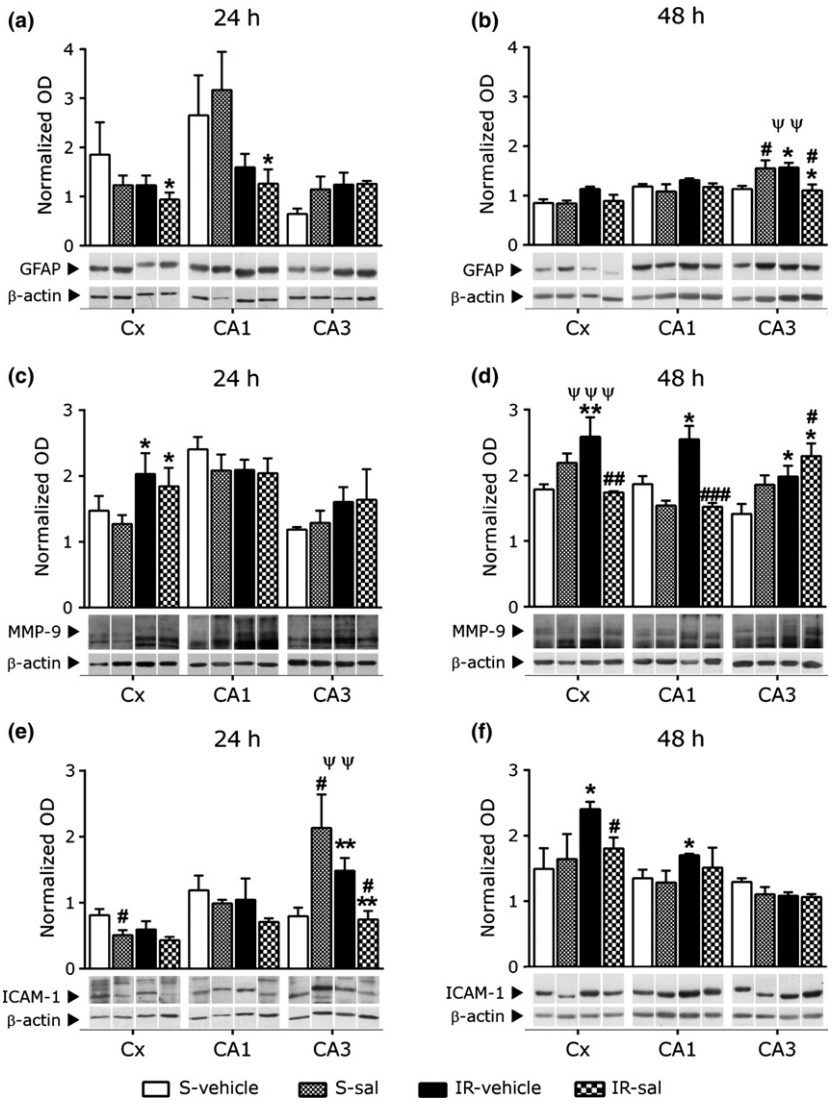

Fig. 3 Effect of IR time and treatment on protein levels of different neurovascular unit components. Representative protein bands of GFAP (50 kDa) at (a) 24 h and (b) 48 h, MMP-9 (87 kDa) at (c) 24 h and (d) 48 h and ICAM-1 (58 kDa) at (e) 24 h and (f) 48 h in the different structures studied. Averages of the densitometric analysis corresponding to five rats (mean ± SEM) normalized with respect to β-actin (40 kDa) are indicated above the bands. Statistics between the different conditions, indicated at the bottom of the image, are represented by *when IR are compared, by #when treatments are compared and by Ψfor significant interactions between IR and treatment. One symbol $p < 0.05$, two symbols $p < 0.01$, three symbols $p < 0.001$, by two-way ANOVA, $n = 5$.

levels were abolished or decreased by the treatment with salubrinal (Fig. 6). Of note, the salubrinal treatment resulted in a tendency to increase these transcripts in CA3 both at 24 h and 48 h that was significant in the comparison between IR-treated and non-treated animals (Fig. 6a and c). No intrinsic effect of salubrinal on these transcripts was observed in sham animals (Fig. 6c and d). Significant interactions between salubrinal treatment and IR were observed for Cx at 24 and 48 h, in CA3 at 24 h, and in CA1 at 48 h.

Cell demise

An IR-induced significant decrease in the number of NeuN-labeled cells was observed in pyramidal layers of CA1, CA3, and Cx. The treatment with salubrinal significantly reduced the neuronal demise only in the CA1 pyramidal layer (Fig. 7a and b).

Discussion

The inflammatory response after global ischemia is structure-dependent

TNF-α levels observed in this study reveal a lower inflammatory response in Cx compared to hippocampus, suggesting that hippocampus would be more prone to sterile inflammation. In addition, the inflammatory response is different in CA3 and CA1. Thus, CA3 presented a faster response that disappeared at 48 h, compared to the delayed and striking response at 48 h observed in CA1. This suggests that the hippocampal sterile inflammation is limited to CA1 and could account for its greater neuronal demise at 7 days, in accordance with the greater ischemic-induced vulnerability described for CA1 (Kirino *et al.* 1985; Petito *et al.* 1987; Zhu *et al.* 2012). Moreover, the treatment with salubrinal brings forward the TNF-α peak in CA1 from 48 to 24 h and

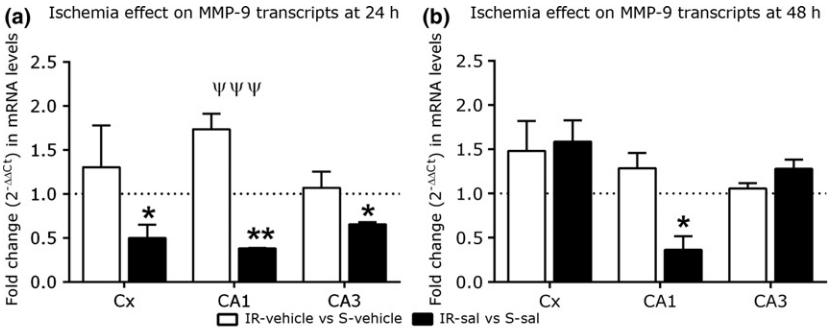

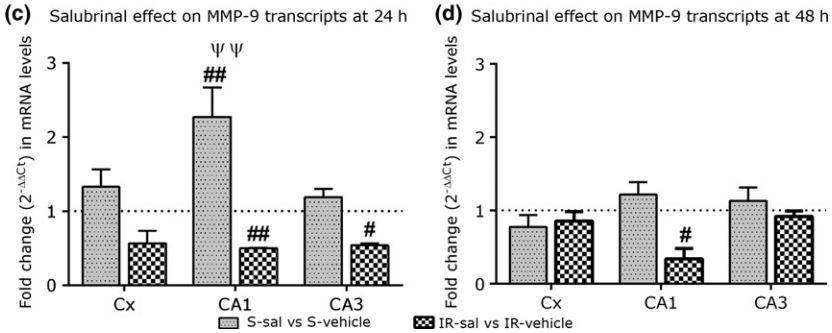

Fig. 4 Effect of IR time and salubrinal treatment on neurovascular unit MMP-9 mRNA levels. Fold changes ($2^{-\Delta\Delta Ct}$) at 24 and 48 h showing the effect of ischemia (a and b) and the effect of salubrinal (c and d) on MMP-9 transcripts. The controls [respective sham animals in (a) and (b), and respective non-treated animals in (c) and (d)] are represented by a value of 1, dotted line. Statistics between the different conditions are represented by *when IR are compared, by #when treatments are compared and a Ψfor significant interactions between IR and treatment. One symbol $p < 0.05$, two symbols $p < 0.01$, three symbols $p < 0.001$, by two-way ANOVA, $n = 5$.

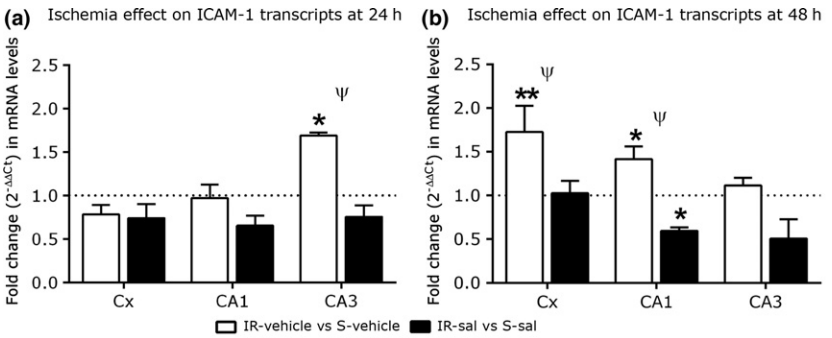

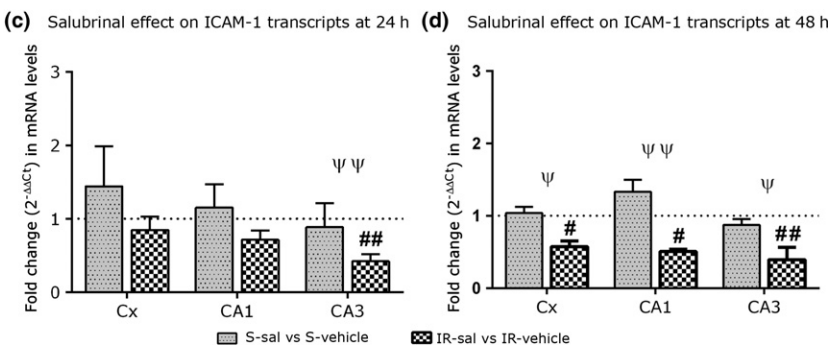

Fig. 5 Effect of IR time and salubrinal treatment on neurovascular unit ICAM-1 mRNA levels. Fold changes ($2^{-\Delta\Delta Ct}$) at 24 and 48 h showing the effect of ischemia (a and b) and the effect of salubrinal (c and d) on ICAM-1transcripts. The controls [respective sham animals in (a) and (b), and respective non-treated animals in (c) and (d)] are represented by a value of 1, dotted line. Statistics between the different conditions are represented by *when IR are compared, by #when treatments are compared and a Ψfor significant interactions between IR and treatment. One symbol $p < 0.05$, two symbols $p < 0.01$, by two-way ANOVA, $n = 5$.

increases the TNF-α levels in CA3 at 24 h, indicating that enhancing UPR-PERK pathway modifies the time course of the inflammation, which would be in agreement with the increases of NF-κB observed at 24 h. Of note, salubrinal acts at a local level and does not modify the inflammation markers in blood, as reveals the lack of response of C-reactive protein in the blood.

UPR inhibits NF-κB activation by inflammatory stimuli (canonical pathway) but ER stress is able to activate NF-κB through the non-canonical pathway, as described in cell culture (Jiang *et al.* 2003; Deng *et al.* 2004). Thus, the similarity in the NF-κB levels in Cx and CA1, despite their striking differences in the TNF-α inflammatory stimulus, suggests an almost exclusively non-canonical expression of NF-κB in Cx, in a

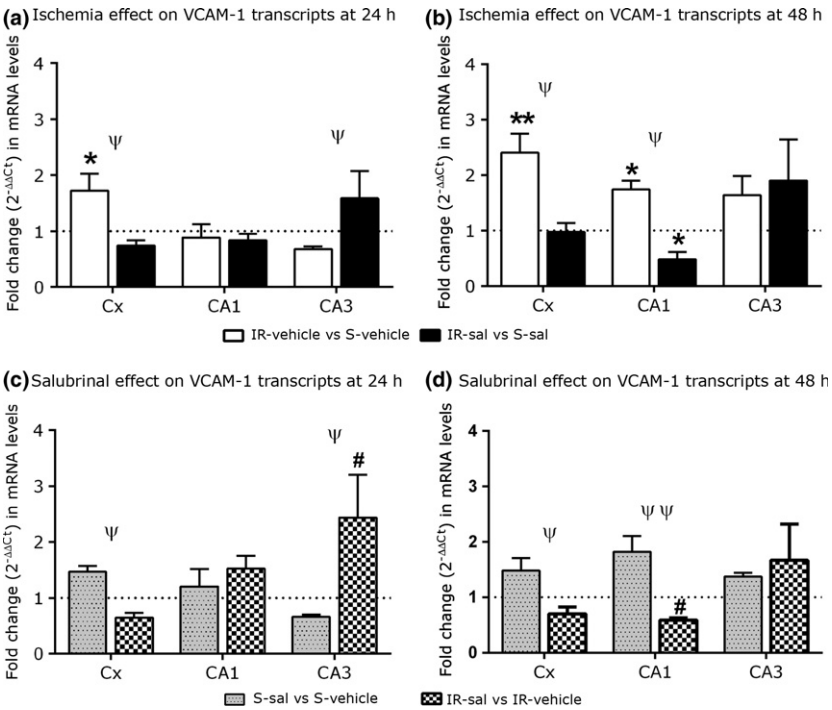

Fig. 6 Effect of IR time and salubrinal treatment on neurovascular unit VCAM-1 mRNA levels. Fold changes ($2^{-\Delta\Delta Ct}$) at 24 and 48 h showing the effect of ischemia (a and b) and the effect of salubrinal (c and d) on VCAM-1 transcripts. The controls [respective sham animals in (a) and (b), and respective non-treated animals in c and d)] are represented by a value of 1, dotted line. Statistics between the different conditions are represented by *when IR are compared, by #when treatments are compared and a Ψfor significant interactions between IR and treatment. One symbol $p < 0.05$, two symbols $p < 0.01$, by two-way ANOVA, $n = 5$.

similar way as reported in cell culture (Nakajima *et al.* 2011). In CA1, NF-κB levels could mirror the balance between the activation of the canonical and non-canonical pathways. Thus, the similarity in NF-κB levels and differences in TNF-α levels support the idea of different inflammatory properties for Cx and CA1, although additional experimental support is required to prove it. In addition, the salubrinal-induced decrease in CA3 NF-κB levels at 24 h contrasts with the later CA1 and Cx decrease (at 48 h), suggesting a delayed response in these structures. The faster IR-dependent increases in CA3 TNF-α levels compared to those in CA1 provides additional support for the idea of different properties in BBB permeability between these structures.

How long lasting is the salubrinal effect? Our data on phosphorylated eIF2α showed a salubrinal-induced enhancement of UPR-PERK pathway at 5 h, in agreement with previous reports (Nakka *et al.* 2010). The inflammatory effect elicited by eIF2α phosphorylation does not require sustained phosphorylation in cell culture (Kitamura 2009) which would agree with our data where eIF2α show similar phosphorylation for treated and non-treated ischemic animals at 24 h. We think that the second dose of salubrinal has no effect on the inflammatory markers, since it resulted in a decrease in NF-κB levels and in TNF-α levels in treated and non-treated IR animals at 48 h.

Different response to ischemia in different cell types of the neurovascular unit

The distinct levels of TNF-α in Cx, CA1, and CA3 reveal local differences in the inflammatory response. These differences also appeared after the salubrinal treatment, adding consistency to the data. It is not clear to what extent the different cells that form the BBB contribute to their local properties and we hypothesized that local inflammatory properties in the different structures mirror not only differences in the neuronal response, but also differences in the neurovascular unit. To prove this hypothesis we studied the ischemic response of the cell types that form the neurovascular unit in different brain structures.

Astrocytes

Following salubrinal treatment, GFAP decreases at 24 h in CA1 and Cx while no changes are detected at 48 h, contrasting with the lack of response at 24 h and the decrease at 48 h in CA3. This supports the idea of a delayed response in CA3 with respect to CA1 and Cx and our hypothesis of local properties for the BBB. In addition, our data together with the lack of response to salubrinal reported at 72 h after spinal cord injury (Ohri *et al.* 2013) suggests that ER stress in astrocytes is limited to a few days rather than a lack of responsiveness.

Pericytes

Pericytes are the main producers of MMP-9 (Takata *et al.* 2011), a typical marker of BBB impairment (Rosenberg *et al.* 1992, 1996; Ueno *et al.* 2009) that in our hands exhibited a general ischemic-induced BBB impairment at 48 h. The early increase in MMP-9 expression and the maintenance of this high expression level in Cx compared with the delayed MMP-9 increase in CA1 suggest that BBB

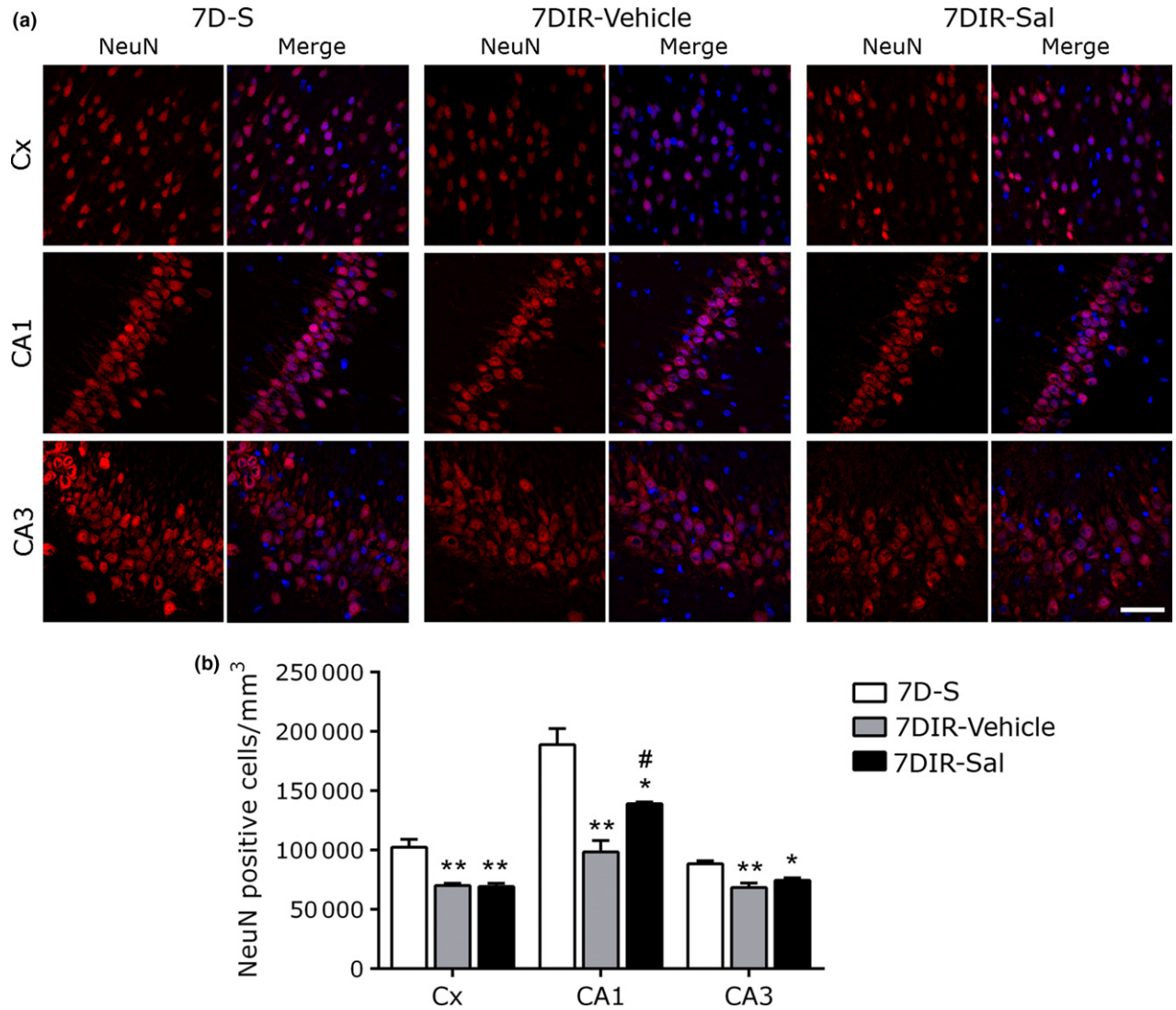

Fig. 7 Neuronal demise after salubrinal treatment. (a) Cortex, CA1 and CA3 labeled with NeuN and with NeuN+4′,6-diamidino-2-phenylindole (DAPI) in the different conditions studied. Bar = 50 μm. (b) Graph shows the number of neurons stained with NeuN in IR non-treated (white columns) and treated (black columns) with salubrinal. Significant differences as a consequence of IR are represented by * and significant differences between treatments are indicated by #. (one symbol $p < 0.05$, two symbols $p < 0.01$, one-way ANOVA, $n = 5$).

damage occurs more rapidly in Cx. Given the reduced vulnerability to ischemia of Cx compared to CA1 (Kirino *et al.* 1985; Petito *et al.* 1987; Zhu *et al.* 2012), the faster peak in Cx MMP-9 expression supports the idea that vulnerability depends on an intrinsic neuronal resistance to ischemia (Tecoma and Choi 1989) rather than a greater protective role of the neurovascular unit in this structure. The different time courses of BBB impairment in the different structures studied also provides support for local inflammatory properties in the neurovascular unit.

Salubrinal treatment was not able to prevent the early BBB impairment observed in Cx; however, its effects on MMP-9 at 48 h reveal two critical aspects: (i) the enhancement of differences between CA1, CA3, and Cx by salubrinal, supporting structure-dependent properties in the neurovascular unit following ischemia, and (ii) the ability of salubrinal to prevent or at least minimize the late BBB impairment in CA1 and Cx. The MMP-9 mRNA levels at 24 h suggest that the response observed in the protein at 48 h has already been elicited 24 h earlier in all the structures studied. The decreased levels of both MMP-9 mRNA and protein in CA1 and Cx after the treatment with salubrinal suggest that the UPR enhancement helps to decrease the BBB impairment. Interestingly, salubrinal was not able to prevent the BBB impairment in CA3 in spite of the ability of this agent to increase the eIF2α phosphorylation.

Endothelial response

Changes in the role of endothelial cells in the properties of the BBB have been related with age. Thus, embryonic neural progenitor cells have been reported as inducers of BBB properties in cerebral endothelial cells (Weidenfeller *et al.* 2007). Also, ICAM-1 and VCAM-1, the key players in the adhesion of circulating blood cells to the endothelium (Norman *et al.* 2008; Li *et al.* 2011), present aging-dependent differences in various brain areas after ischemic insult (Anuncibay-Soto *et al.* 2014). Here, we show that structural differences in the endothelial cells also appear in young adult animals. Therefore, local differences in expression and time course of adhesion molecules support a role for endothelial cells in local differences in the neurovascular unit in response to the ischemic insult.

The time-course pattern of MMP-9 expression after the ischemic insult seemed to be delayed 24 h with respect to that observed for ICAM-1, suggesting an increased adhesion between endothelium and circulating blood cells at 48 h in CA1 and Cx. The treatment with salubrinal also reproduced the delayed time-course of expression for these molecules. Therefore, the consecutive steps played by these molecules in BBB impairment, described for middle cerebral artery occlusion (Wang *et al.* 2007) also appear in global ischemia.

Ischemia-induced changes in ICAM-1 expression in CA3 appeared 24 h earlier than in Cx and CA1. This is corroborated by the VCAM-1 increase in CA3 at 24 h after salubrinal treatment, contrasting with its decreased or absent effects on Cx and CA1. This provides additional support for differences in adhesion properties between CA3 and the other structures studied. Therefore, all the markers here analyzed are consistent and reinforce the idea that, following ischemia, the neurovascular unit in CA3 presents different properties than in CA1 and Cx. Further studies are necessary to determine if these differences also exist in naive animals or are a consequence of ischemic insult.

Neuroprotective role of post-ischemic UPR-PERK pathway modulation

Treatment with salubrinal decreased the levels of both CAMs and MMP-9 in CA1 and Cx, giving credence to the ideas that (i) a reduction in leukocyte transmigration would help to reduce BBB impairment and (ii) the neuroprotective role of salubrinal involves the inflammatory response. This molecular correlation is not clear in CA3 but contributes to the hypothesis of differences in neurovascular unit properties following ischemia between different brain structures.

Is the salubrinal treatment helpful for neuronal protection? The reduction in neuronal demise in CA1 7 days after injury in salubrinal-treated animals and the decrease in BBB impairment (measured as MMP-9 levels and supported by the rest of molecules here studied) support a neuroprotective effect for this agent, involving crosstalk between the inflammatory response and UPR. The smaller UPR response in CA1 using a global ischemia model (Llorente *et al.* 2013) suggests a reduced ability of CA1 to ignite the UPR that could be compensated by the salubrinal treatment. This reduced UPR could explain its greater vulnerability to ischemia and salubrinal would neuroprotect CA1 by promoting its limited UPR which in turn, would modify the inflammatory response.

In accordance with the idea of the dual role of inflammation, both protective and deleterious (Ceulemans *et al.* 2010), the comparable and strikingly high levels of TNF-α at 48 h in both treated and non-treated animals suggests that levels of sterile inflammation have been reached at 48 h in the hippocampus. Since salubrinal was able to increase inflammation at 24 h followed by reducing the BBB impairment at 48 h, we think that the effect of salubrinal on inflammation at 24 h is still protective.

Conclusion

In conclusion, this study shows that salubrinal treatment presents a neuroprotective role in CA1. We suggest that CA1 presents a limited UPR against the ischemia and salubrinal treatment enhances this response thus reducing the cell delayed mortality. We also suggest that the neurovascular unit presents structure-dependent inflammatory properties to ischemic injury and differences in the time course of the inflammatory response for CA1/Cx and CA3, which is also supported by the salubrinal treatment. In addition, our study demonstrates the responsiveness of endothelial cells and, to a much lesser degree, of astrocytes to the salubrinal treatment. Therefore, the salubrinal treatment affects different cell populations in different ways, resulting in local rather than systemic effects. Finally, this study demonstrates that UPR modulators are able to modify the inflammatory response. The effectiveness of salubrinal when administered after the ischemic insult suggest therapeutic possibilities for UPR modulators in stroke that, up to date, have not been taken into account.

Acknowledgments and conflict of interest disclosure

We thank Ana Isabel Cortina Rivero and Manuel García Gómez, Department of Surgery (University of Leon) for surgical collaboration. This study was supported by MINECO (reference BIO2013-49006-C2-2-R), which also supports Berta Anuncibay-Soto and María Santos-Galdiano by fellowships. Enrique Font is supported by the University of León. Diego Pérez Rodríguez has a grant from Junta de Castilla y León (EDU/346/2013). We also thank Covidien Neurovascular for additional financial support. The authors have no conflict of interest to declare.

All experiments were conducted in compliance with the ARRIVE guidelines.

References

Aarts M., Iihara K., Wei W. L., Xiong Z. G., Arundine M., Cerwinski W., MacDonald J. F. and Tymianski M. (2003) A key role for TRPM7 channels in anoxic neuronal death. *Cell* **115**, 863–877.

Anuncibay-Soto B., Perez-Rodriguez D., Llorente I. L., Regueiro-Purrinos M., Gonzalo-Orden J. M. and Fernandez-Lopez A. (2014) Age-dependent modifications in vascular adhesion molecules and apoptosis after 48-h reperfusion in a rat global cerebral ischemia model. *Age (Dordr)*. **36**, 9703-014-9703-7. Epub 2014 Sep 3.

Boyce M., Bryant K. F., Jousse C. *et al.* (2005) A selective inhibitor of eIF2alpha dephosphorylation protects cells from ER stress. *Science* **307**, 935–939.

Ceulemans A. G., Zgavc T., Kooijman R., Hachimi-Idrissi S., Sarre S. and Michotte Y. (2010) The dual role of the neuroinflammatory response after ischemic stroke: modulatory effects of hypothermia. *J. Neuroinflammation* **7**, 74-2094-7-74.

Corps K. N., Roth T. L. and McGavern D. B. (2015) Inflammation and neuroprotection in traumatic brain injury. *JAMA Neurol.* **72**, 355–362.

Deng J., Lu P. D., Zhang Y., Scheuner D., Kaufman R. J., Sonenberg N., Harding H. P. and Ron D. (2004) Translational repression mediates activation of nuclear factor kappa B by phosphorylated translation initiation factor 2. *Mol. Cell. Biol.* **24**, 10161–10168.

Doll D. N., Hu H., Sun J., Lewis S. E., Simpkins J. W. and Ren X. (2015) Mitochondrial crisis in cerebrovascular endothelial cells opens the blood-brain barrier. *Stroke* **46**, 1681–1689.

Donnan G. A., Fisher M., Macleod M. and Davis S. M. (2008) *Stroke. Lancet.* **371**, 1612–1623.

Fernandez J., Yaman I., Sarnow P., Snider M. D. and Hatzoglou M. (2002) Regulation of internal ribosomal entry site-mediated translation by phosphorylation of the translation initiation factor eIF2alpha. *J. Biol. Chem.* **277**, 19198–19205.

Gundersen H. J., Bagger P., Bendtsen T. F., Evans S. M., Korbo L., Marcussen N., Moller A., Nielsen K., Nyengaard J. R. and Pakkenberg B. (1988) The new stereological tools: disector, fractionator, nucleator and point sampled intercepts and their use in pathological research and diagnosis. *APMIS.* **96**, 857–881.

Halterman M. W., De Jesus C., Rempe D. A., Schor N. F. and Federoff H. J. (2008) Loss of c/EBP-beta activity promotes the adaptive to apoptotic switch in hypoxic cortical neurons. *Mol. Cell Neurosci.* **38**, 125–137.

Harding H. P., Zhang Y., Bertolotti A., Zeng H. and Ron D. (2000) Perk is essential for translational regulation and cell survival during the unfolded protein response. *Mol. Cell* **5**, 897–904.

Hasnain S. Z., Lourie R., Das I., Chen A. C. and McGuckin M. A. (2012) The interplay between endoplasmic reticulum stress and inflammation. *Immunol. Cell Biol.* **90**, 260–270.

Hawkins B. T. and Davis T. P. (2005) The blood-brain barrier/neurovascular unit in health and disease. *Pharmacol. Rev.* **57**, 173–185.

Jiang H. Y., Wek S. A., McGrath B. C., Scheuner D., Kaufman R. J., Cavener D. R. and Wek R. C. (2003) Phosphorylation of the alpha subunit of eukaryotic initiation factor 2 is required for activation of NF-kappaB in response to diverse cellular stresses. *Mol. Cell. Biol.* **23**, 5651–5663.

Jin R., Yang G. and Li G. (2010) Inflammatory mechanisms in ischemic stroke: role of inflammatory cells. *J. Leukoc. Biol.* **87**, 779–789.

Joussen A. M., Doehmen S., Le M. L., Koizumi K., Radetzky S., Krohne T. U., Poulaki V., Semkova I. and Kociok N. (2009) TNF-alpha mediated apoptosis plays an important role in the development of early diabetic retinopathy and long-term histopathological alterations. *Mol. Vis.* **15**, 1418–1428.

Kaufman R. J. (1999) Stress signaling from the lumen of the endoplasmic reticulum: coordination of gene transcriptional and translational controls. *Genes Dev.* **13**, 1211–1233.

Kirino T., Tamura A. and Sano K. (1985) Selective vulnerability of the hippocampus to ischemia–reversible and irreversible types of ischemic cell damage. *Prog. Brain Res.* **63**, 39–58.

Kitamura M. (2009) Biphasic, bidirectional regulation of NF-kappaB by endoplasmic reticulum stress. *Antioxid. Redox Signal.* **11**, 2353–2364.

Li J., Wang J. J. and Zhang S. X. (2011) Preconditioning with endoplasmic reticulum stress mitigates retinal endothelial inflammation via activation of X-box binding protein 1. *J. Biol. Chem.* **286**, 4912–4921.

Livak K. J. and Schmittgen T. D. (2001) Analysis of relative gene expression data using real-time quantitative PCR and the 2(-Delta Delta CT)) Method. *Methods* **25**, 402–408.

Llorente I. L., Burgin T. C., Perez-Rodriguez D., Martinez-Villayandre B., Perez-Garcia C. C. and Fernandez-Lopez A. (2013) Unfolded protein response to global ischemia following 48 h of reperfusion in the rat brain: the effect of age and meloxicam. *J. Neurochem.* **127**, 701–710.

Nakajima S. and Kitamura M. (2013) Bidirectional regulation of NF-kappaB by reactive oxygen species: a role of unfolded protein response. *Free Radic. Biol. Med.* **65**, 162–174.

Nakajima S., Hiramatsu N., Hayakawa K., Saito Y., Kato H., Huang T., Yao J., Paton A. W., Paton J. C. and Kitamura M. (2011) Selective abrogation of BiP/GRP78 blunts activation of NF-kappaB through the ATF6 branch of the UPR: involvement of C/EBPbeta and mTOR-dependent dephosphorylation of Akt. *Mol. Cell. Biol.* **31**, 1710–1718.

Nakka V. P., Gusain A. and Raghubir R. (2010) Endoplasmic reticulum stress plays critical role in brain damage after cerebral ischemia/reperfusion in rats. *Neurotox. Res.* **17**, 189–202.

Nakka V. P., Prakash-Babu P. and Vemuganti R. (2014) Crosstalk between endoplasmic reticulum stress, oxidative stress, and autophagy: potential therapeutic targets for acute CNS injuries. *Mol. Neurobiol.* **53**, 532–544.

Norman M. U., James W. G. and Hickey M. J. (2008) Differential roles of ICAM-1 and VCAM-1 in leukocyte-endothelial cell interactions in skin and brain of MRL/faslpr mice. *J. Leukoc. Biol.* **84**, 68–76.

Ohri S. S., Hetman M. and Whittemore S. R. (2013) Restoring endoplasmic reticulum homeostasis improves functional recovery after spinal cord injury. *Neurobiol. Dis.* **58**, 29–37.

Paxinos G. and Watson C. (1996) *The Rat Brain in Stereotaxic Coordinates*. Academic Press, San Diego.

Petito C. K., Feldmann E., Pulsinelli W. A. and Plum F. (1987) Delayed hippocampal damage in humans following cardiorespiratory arrest. *Neurology* **37**, 1281–1286.

Posada-Duque R. A., Barreto G. E. and Cardona-Gomez G. P. (2014) Protection after stroke: cellular effectors of neurovascular unit integrity. *Front. Cell. Neurosci.* **8**, 231.

Rius J., Guma M., Schachtrup C., Akassoglou K., Zinkernagel A. S., Nizet V., Johnson R. S., Haddad G. G. and Karin M. (2008) NF-kappaB links innate immunity to the hypoxic response through transcriptional regulation of HIF-1alpha. *Nature* **453**, 807–811.

Rosenberg G. A., Kornfeld M., Estrada E., Kelley R. O., Liotta L. A. and Stetler-Stevenson W. G. (1992) TIMP-2 reduces proteolytic opening of blood-brain barrier by type IV collagenase. *Brain Res.* **576**, 203–207.

Rosenberg G. A., Navratil M., Barone F. and Feuerstein G. (1996) Proteolytic cascade enzymes increase in focal cerebral ischemia in rat. *J. Cereb. Blood Flow Metab.* **16**, 360–366.

Rubovitch V., Barak S., Rachmany L., Goldstein R. B., Zilberstein Y. and Pick C. G. (2015) The neuroprotective effect of salubrinal in a

mouse model of traumatic brain injury. *Neuromolecular Med.* **17**, 58–70.

Schroder M. (2008) Endoplasmic reticulum stress responses. *Cell. Mol. Life Sci.* **65**, 862–894.

Schroder M. and Kaufman R. J. (2005) The mammalian unfolded protein response. *Annu. Rev. Biochem.* **74**, 739–789.

Takata F., Dohgu S., Matsumoto J. *et al.* (2011) Brain pericytes among cells constituting the blood-brain barrier are highly sensitive to tumor necrosis factor-alpha, releasing matrix metalloproteinase-9 and migrating in vitro. *J. Neuroinflammation* **8**, 106-2094-8-106.

Taylor S., Wakem M., Dijkman G., Alsarraj M. and Nguyen M. (2010) A practical approach to RT-qPCR-Publishing data that conform to the MIQE guidelines. *Methods* **50**, S1–S5.

Tecoma E. S. and Choi D. W. (1989) GABAergic neocortical neurons are resistant to NMDA receptor-mediated injury. *Neurology* **39**, 676–682.

Ueno M., Wu B., Nishiyama A., Huang C. L., Hosomi N., Kusaka T., Nakagawa T., Onodera M., Kido M. and Sakamoto H. (2009) The expression of matrix metalloproteinase-13 is increased in vessels with blood-brain barrier impairment in a stroke-prone hypertensive model. *Hypertens. Res.* **32**, 332–338.

Vieira M., Fernandes J., Carreto L., Anuncibay-Soto B., Santos M., Han J., Fernandez-Lopez A., Duarte C. B., Carvalho A. L. and Santos A. E. (2014) Ischemic insults induce necroptotic cell death in hippocampal neurons through the up-regulation of endogenous RIP3. *Neurobiol. Dis.* **68**, 26–36.

Walter P. and Ron D. (2011) The unfolded protein response: from stress pathway to homeostatic regulation. *Science* **334**, 1081–1086.

Wang Q., Tang X. N. and Yenari M. A. (2007) The inflammatory response in stroke. *J. Neuroimmunol.* **184**, 53–68.

Weidenfeller C., Svendsen C. N. and Shusta E. V. (2007) Differentiating embryonic neural progenitor cells induce blood-brain barrier properties. *J. Neurochem.* **101**, 555–565.

World Health Organization (WHO) (2011) *The top ten causes of death*. Fact sheet number, WHO, Geneva.

Xue X., Piao J. H., Nakajima A., Sakon-Komazawa S., Kojima Y., Mori K., Yagita H., Okumura K., Harding H. and Nakano H. (2005) Tumor necrosis factor alpha (TNFalpha) induces the unfolded protein response (UPR) in a reactive oxygen species (ROS)-dependent fashion, and the UPR counteracts ROS accumulation by TNFalpha. *J. Biol. Chem.* **280**, 33917–33925.

Yilmaz G. and Granger D. N. (2010) Leukocyte recruitment and ischemic brain injury. *Neuromolecular Med.* **12**, 193–204.

Zarow C., Vinters H. V., Ellis W. G., Weiner M. W., Mungas D., White L. and Chui H. C. (2005) Correlates of hippocampal neuron number in Alzheimer's disease and ischemic vascular dementia. *Ann. Neurol.* **57**, 896–903.

Zhang K. and Kaufman R. J. (2008) From endoplasmic-reticulum stress to the inflammatory response. *Nature* **454**, 455–462.

Zhu H., Yoshimoto T., Imajo-Ohmi S., Dazortsava M., Mathivanan A. and Yamashima T. (2012) Why are hippocampal CA1 neurons vulnerable but motor cortex neurons resistant to transient ischemia? *J. Neurochem.* **120**, 574–585.

